Settlement Evaluation of a Concrete Face Rock-Fill Dam (CFRD) Using a Back-Analysis Method Based on Measurement Results (A Case Study of Siah-Bisheh Dam)

Mohammad Ali Abedian[1], Farhang Farrokhi[2] & Reza Rasouli[2,*]

[1]Department of Civil Engineering, Mazandaran Regional Water Co., Savadkooh, Iran
[2]Civil Engineering Department, Faculty of Engineering, University of Zanjan, Zanjan, Iran
*E-mail: Reza.rasouli255@gmail.com

Abstract. The behavior of the Siah-Bisheh concrete face rock-fill dam in Mazandaran, Iran was investigated. Numerical analyses were performed before construction to evaluate the stability and predict the deformation of the dam. The material properties were chosen based on the results of geotechnical investigations. The amounts for deformation and settlement of the concrete surface were also calculated with the numerical model. The information from a number of geotechnical instruments was collected after construction and analyzed to measure settlement at different sections of the dam. The locations of the different deformations and their values are presented with various contours. The data were analyzed and used to revise the original numerical model of the dam. Following that, the long-term stability of the dam was evaluated, using parameters that were modified based on the measurement data. A comparison of the results from the numerical analysis and the values obtained from the dam settlement measurement showed that the initial results from the numerical model were much higher than the real values. It also showed that the number of construction layers used in the modeling of the dam had a significant effect on the obtained maximum amount of deformation.

Keywords: *back analysis; concrete-face rock-fill dam (CFRD); instrumentation; settlement; Siah-Bisheh Dam.*

1 Introduction

Concrete-face rock-fill dams (CFRDs) are now constructed in considerable numbers throughout the world [1,2]. Over the past two decades, many CFRDs higher than 150 m and up to 240 m were built, such as the 233 m-high Shuibuya Dam and the 179 m-high Hongjiadu Dam in China [3,4]. In CFRDs, the concrete slab plays an important role as an impervious membrane and any cracks in the slab would impair the integrity of the seepage control system and weaken the structure or even threaten the safety of the dam [5] (e.g. the failure of Gouhou CFRD in China in August, 1993 [6]). However, deformation of the concrete face slab depends on the deformation of the rock-fill dam due to its

Received May 6th, 2018, 1st Revision July 31st, 2018, 2nd Revision August 7th, 2018, Accepted for publication September 12th, 2018.
 ISSN: 2337-5779, DOI: 10.5614/j.eng.technol.sci.2018.50.4.5

poor resistance to deformation. Excessive deformation of rock-fill after the completion of the concrete face slab will cause separation between the slabs and the cushion layer or even cracks in the slab [7,8]. In order to reduce this potential risk in high CFRDs it is necessary to understand the deformation characteristics of rock-fill dams in order to make the rock-fill compatible with the concrete face to reduce the amount of cracks in the slab, and to improve the design of high CFRDs. In the design stage of a CFRD, various numerical methods, such as finite element method (FEM), are used to predict the deformation and stress on the basis of the geomechanical parameters obtained from laboratory tests [4]. However, due to the scale effect and other factors, the in-situ geo mechanical properties of rock-fill may differ from those determined by laboratory tests [9,10].

Therefore, in order to better understand the dam deformation property, both deformation monitoring analysis and back-analysis are required. Deformation monitoring is an effective method for analyzing the deformation characteristics of a dam, providing a warning system for abnormal behavior of the dam [5,11]. It is also helpful to understand the mechanism of deformation [12-14]. A comparison of the observed deformations with those obtained from FEM is necessary to verify the safety of a structure as well as the design parameters [13]. Furthermore, in-depth studies of such comparisons are highly useful to gain experience for future applications [12]. However, because the history of high CFRDs is not very long, comparisons between predicted (FEM) and observed deformations are rare in the literature. For this reason, it is significant to study the deformation characteristics of extra high CFRDs.

This paper reports the analysis of actual measured deformations resulting from continuous monitoring of the Siah-Bisheh CFRD in Mazandaran, Iran. A displacement back-analysis for parameters was performed using FEM. The long-term deformation of the dam was predicted on the basis of the parameters obtained from the back-analysis. This analysis focuses on displacements and the available monitoring data over several years, covering the construction phase and the first stage of filling of the reservoir. The FE simulation in the back-analysis was conducted in some two-dimensional plain-strain conditions. Depending on the time of deformation, the process of construction and water storage were simulated as realistically as possible.

Back-analyzed soil parameters can be used in deformation and stress analyses of CFRD during construction and operation, which is beneficial to CFRD safety operation, seismic safety assessment, and enforcement design. Because the mechanical properties involved are complex, soil constitutive models are strongly nonlinear. It is difficult to directly calculate the soil parameters by inverting the CFRD FEM displacement calculation. Thus, displacement back-

analysis is applied by optimizing the soil parameters. The deviation between the calculated CFRD displacements and the prototype monitoring values becomes an objective function. The optimal values of the soil parameters to be determined are progressively approximated through iteration by minimizing the fitness values of the objective function. During soil parameter optimization, time-consuming FEM calculations are frequently performed; thus, the rate of convergence is slow and the back-analysis fails to function effectively for larger-scale problems. Most previous studies concentrated on the behavior of CFRD posited at the end of the construction and evaluated different methods to predict the amount of settlement and deformation of the domain body and the concrete face at the end of the impounding. In this study, however, the focus was mainly on the appropriate implementation of the collected measurement data with regard to evaluation of the long-term stability of the dam. The Siah-Bisheh concrete face rock-fill dam located in the northern part of Iran was investigated as a case study. At the time of writing, this study was the first of its kind in Iran.

2 Introduction to Siah-Bisheh Dam

Siah-Bisheh Dam and its pump storage power plant is located 125 km north of Tehran, in Mazandaran province, Iran. The dam site is located near the village of Siah-Bisheh, including a pump storage power plant and a high concrete face rock-fill dam (Figure 1). The project aimed to deliver 1040 MW of electricity during peak demand of the electricity network. The dam was built as a balancing system and a hydroelectric power plant, and consists of an upper dam and a lower dam. In the present study, the lower dam was selected for the case study. The lower dam is addressed as 'Siah-Bisheh Dam' in the rest of this paper. The general specifications of the dam are shown in Table 1. Figure 2 shows a cross-section of the dam.

Figure 1 Location of the lower Siah-Bisheh CFRD.

Table 1 General specifications of Siah-Bisheh Dam.

Height	101.00 m
Crest elevation	1911.50 m
Crest length	330.00 m
Crest width	12.00 m
Width of dam in foundation	360.00 m
Upstream slope	1:1.60 (V:H)
Downstream slope	1:1.45 (V:H)

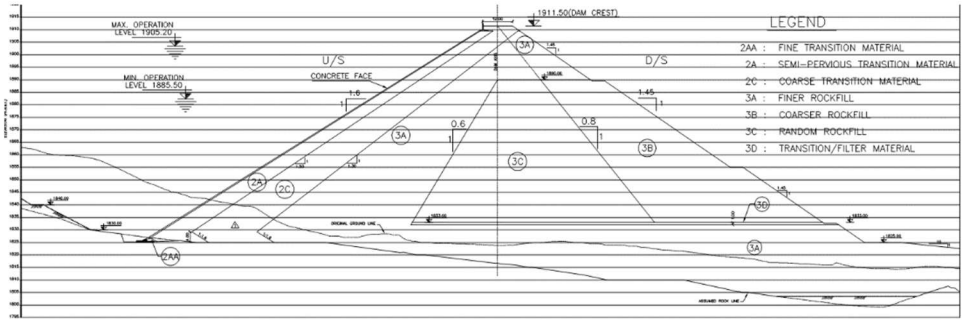

Figure 2 Cross-Section of Siah-Bisheh Dam.

3 Instrumentation

3.1 Installation

Various instruments were installed at different locations on the dam's main body to study the behavior of the dam during construction and impounding, and for long-term monitoring. Among several different behaviors, the deformation of the concrete face and the flow of water in the dam were of the most interest. This was to check the integrity of the concrete face and also to monitor the drainage of water through the foundation of the dam.

The instrumentation used to assist the researchers in monitoring and studying the dam measured the following parameters:

1. Deformation of dam body
2. Deformation of concrete face
3. Movement of peripheral joints and joints between concrete slabs
4. Piezo metric level in dam body and foundation
5. Amount of drained water (Q)
6. Location of drained water along the Plinth
7. Seismic action

The main three instrument sections, placed in a perpendicular direction towards the axis of the dam, were respectively located at kilometers 0+192, 0+272 and 0+352 along the dam crest. The instruments were mainly installed within the dam body at elevations of 1850 m, 1870 m and 1890 m above sea level. Figure 3 shows the instruments installed in section 0+272 of the dam (main section).

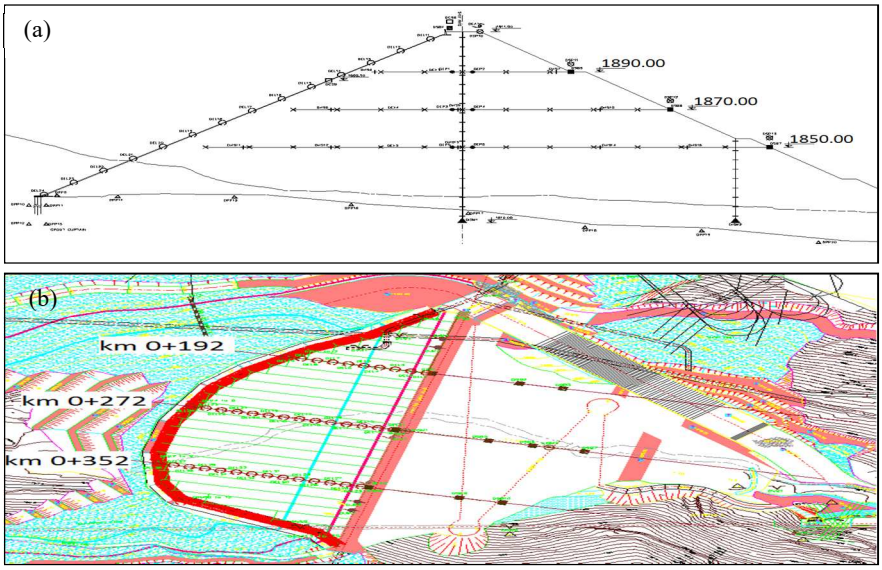

Figure 3 Instrumentation in section 0+272 of the dam: (a) elevation view, (b) plan view.

3.2 Vertical Deformation

The vertical deformation of the dam at different locations was measured by the magnetic settlement plates that were installed at 3-m intervals along the dam. Hydraulic settlement gauges were also installed, at elevations of 1850 m, 1870 m and 1890 m. The recorded data showed very reasonable and acceptable values of settlement. Figure 4 shows data obtained by hydraulic settlement gauges from DHS 11 to DHS15 as well as data from magnetic settlement plate DISM1, as examples. The total amount of settlement one year after completion of the dam body is shown in Figure 5.

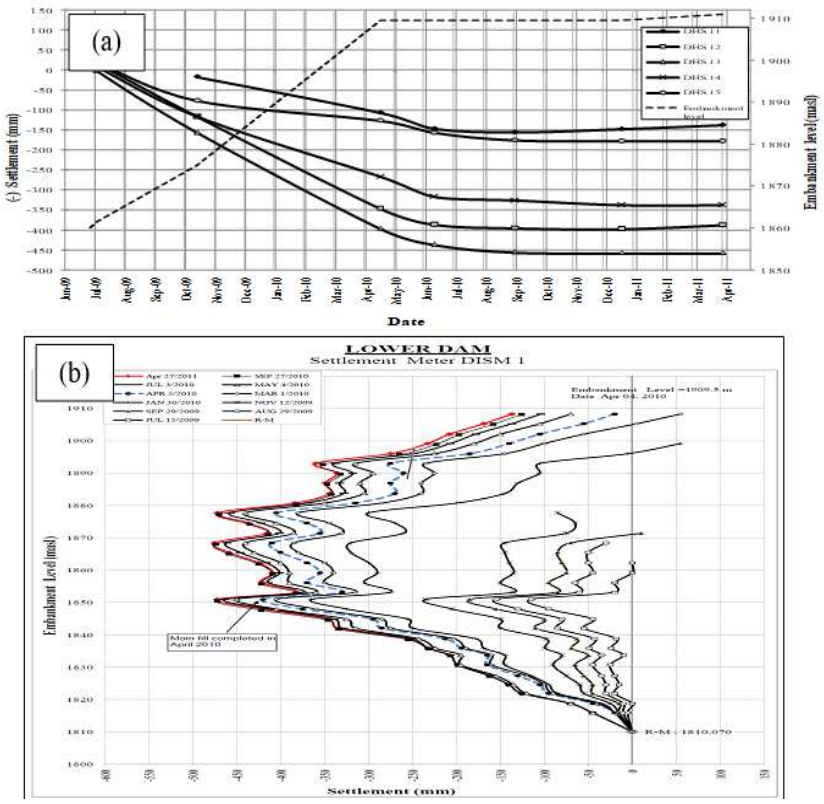

Figure 4 Vertical settlement of the dam: (a) data from hydraulic settlement gauges DHS 11 to DHS15, (b) data from DISM1 magnetic settlement gauges.

It can be seen that there is good agreement between the hydraulic and the magnetic settlement gauges. It can also be seen that the maximum vertical settlement at the end of construction was recorded by instruments installed in the middle section of the dam. This settlement was about 45 cm and occurred at about 0.5H (H is the height of the dam). The data show that most of the recorded settlement occurred due to weight of the upper layers of soil added during construction. These observations are consistent with the researcher's expectations.

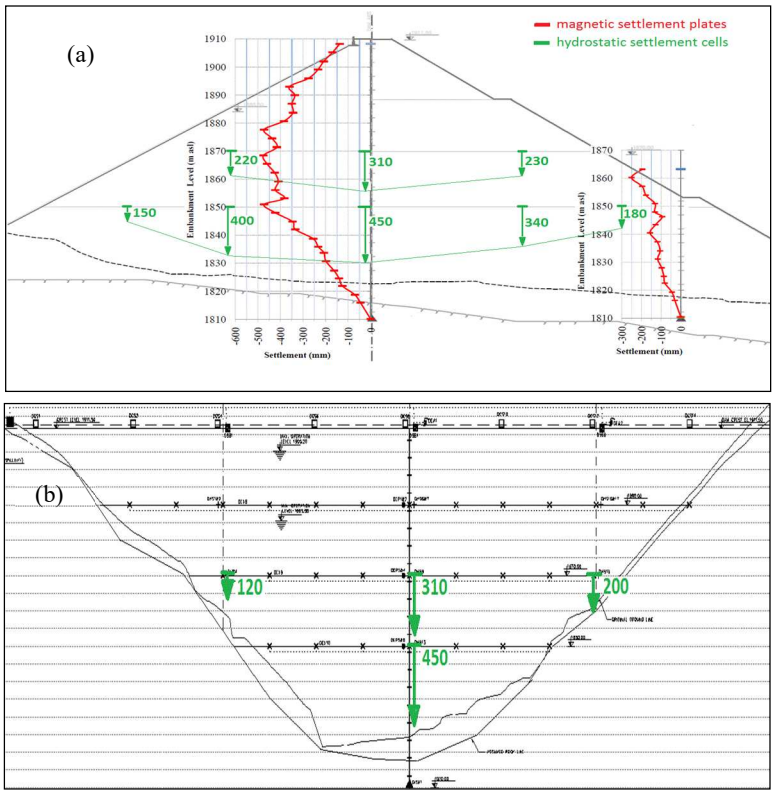

Figure 5 Total settlement recorded one year after completion of construction (a) at section 0+272, (b) longitudinal section.

3.3 Horizontal deformation

Horizontal extensometers were mounted at three different elevations (1850 m, 1870 m and 1890 m) along three different cross sections and one longitudinal section to measure the horizontal deformation of the dam body. The obtained values of horizontal deformation can be summarized as follows:

1. The obtained values of horizontal deformation were mostly small (0.1 to 0.3 percent strain). The horizontal deformation values were between 5 to 15 percent of the vertical deformation values.
2. Rock-fill on the left and right abutment of the dam body deformed horizontally toward the center of the dam's body. The maximum horizontal deformation value of the valley was 6.5 cm, which occurred at 0.3*H*, near the right abutment of the dam. The obtained values of horizontal deformation in the middle section of the dam and along the longitudinal

dam axis are shown in Figure 6. Note that in this figure positive values represent disruption while negative values represent compression.

4 Back-Analysis and Numerical Modeling

To study the settlement of the dam and predict the long-term behavior of the structure, a numerical model of the dam was created using a finite element method. For this purpose, the dam was modeled based on rock-fill properties and parameters that were obtained from the site investigation report and that were used in the primary dam design. These parameters were then revised in accordance with the results of the measurements, after which the final model was created.

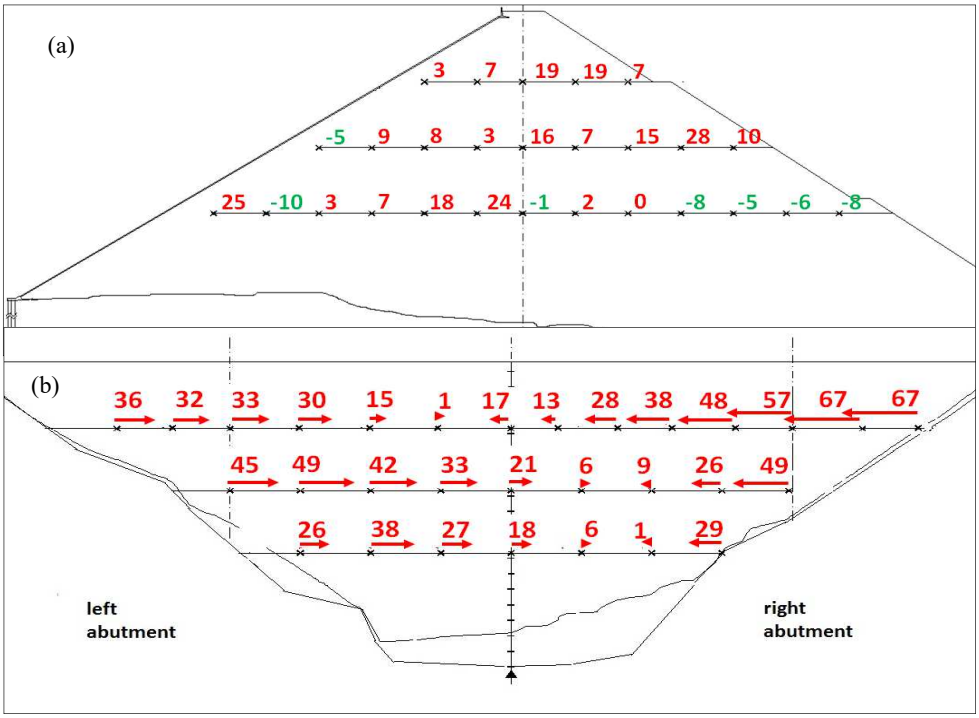

Figure 6 Horizontal deformation values of the dam in mm (a) at section 0+272, (b) along the axis of the dam.

The behavioral model used in the analysis for both the materials of the dam body and the foundation was the elasto-plastic Mohr-Coulomb model. The concrete surface materials were, however, modeled by solid elastic behavior (Jesmani, *et al.* [14]). The properties of the different sections of the dam that were used in the initial model are shown in Table 2. In this table E is the

modulus of elasticity, c is the cohesion, ϕ is the internal friction angle, γ is the unit weight, and v is the Poisson ratio.

After the first analysis was completed, the values shown in Table 2 were revised to obtain settlements closer to the values recorded by the instrumentation. The analyses were repeated a number of times until the desired values were obtained.

Table 2 Initial specifications of numerical modeling.

Zone	Behavior model	E (MPa)	c (kPa)	ϕ°	γ $(\frac{kN}{m^3})$	v
2A	E-P*	59	0	42	22.9	0.30
2B	E-P*	45	0	45	22.2	0.30
3A	E-P*	45	0	45	22.2	0.30
3B	E-P*	45	0	45	22.2	0.30
3C	E-P*	30	0	40	21.8	0.30
Alluvial	E-P*	16	0	28	20.9	0.35
Concrete	Elastic	5000	-	-	25.0	0.20

The load that was applied to the static model was taken into account for both the body weight and the burden of impounding. The body weight was applied to the model gradually and in 15 stages, using the staged modeling technique. This aimed to model the construction phase of the dam in a more accurate manner. In the sixteenth stage, the load of the concrete surface was applied to the dam body and the model reached equilibrium. For the materials located under the water level, the saturated unit weight was considered. Then, the load from impounding upstream water was applied to the concrete surface as hydrostatic pressure.

5 Preliminary Numerical Analysis – Initial Model

To study the effects of impounding, deformation of the concrete surface was obtained from the numerical model before and after applying the impounding load. Figure 7 shows the vertical deformation contours at the end of construction and before impounding in the numerical analysis using the initial specifications of the materials. As can be seen from the figure, the maximum settlement at the end of the dam construction (fifteen stages of analysis) was predicted to be about 90 cm.

By comparing this value with the value of the maximum deformation collected from the measurements (45 cm) it can be seen that the maximum amount of deformation obtained from the numerical model was about twice the observed

values. This shows that the elastic modulus values considered for the numerical modeling were very conservative and smaller than the real behavior of the soil.

Figure 8 shows the amount of vertical deformation of the dam that was calculated by the numerical analysis presented in the originally reported design of the dam. The predicted maximum settlement was calculated to be equal to 120 cm. This high value is mainly because of the fact that burden load was applied in only 6 stages, rather than the 15 stages that were used in the numerical model of this study. It can be seen that modeling the construction phase was very accurate and applying the burden load in a number of stages was critical. In the case of this study this resulted in deformations that could reach up to 30 cm.

To find the most suitable number of loading stages, a separate set of analyses was performed. Various models with different loading stages were analyzed and it was found that increasing the number of layers (loading stages) to more than 15 does not lead to a significant increase in accuracy while it does increase the time consumed of the analysis.

It can also be seen in Figure 7 that the maximum settlement of the dam body occurs in the middle level of the dam body. This can be due to the fact that the settlement of each level is associated with the strain of the underlay and the tension of the upper layer, which are both associated with the height of the settlement level. Therefore, the settlement at any level will contribute to the settlement of the middle of the dam.

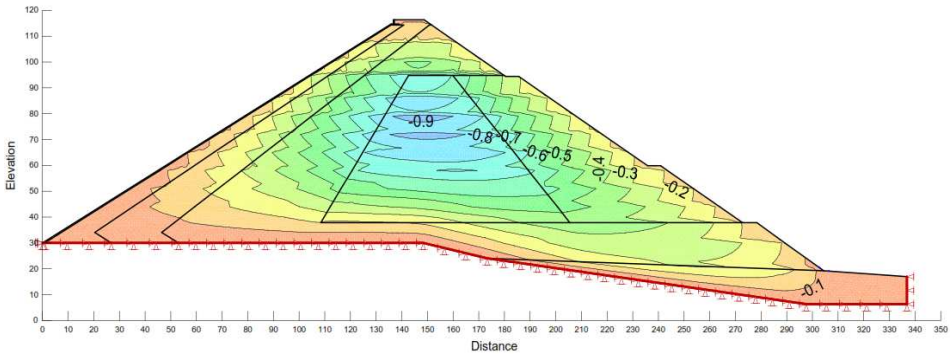

Figure 7 Deformation at the end of construction obtained from numerical analysis using the information of the initial specification of materials (15 loading stages).

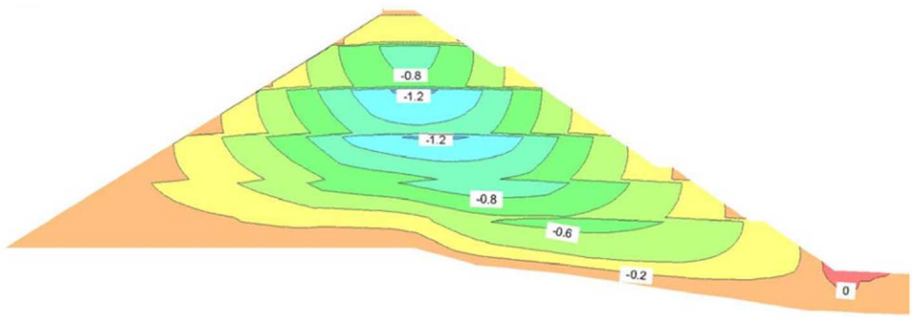

Figure 8 Deformation at the end of construction presented in the original dam design report (initial specification of materials and 6 loading stages).

6 Study of Elastic Modulus

As was shown in the previous section there are significant differences between the results obtained from the measurements and the results of the numerical analysis, where the dam was modeled with the soil properties estimated from the geotechnical investigation report, prepared before construction. The main focus of this paper is on the short-term settlement of a CFRD. CFRDs are generally constructed in different sections, using rock-fill materials. The main settlement mechanism that occurs on rock-fill materials is generally elastic settlement, which has a direct relationship with the modulus of elasticity. Therefore, it is necessary to modify the value of the elastic modulus of the soil to create a better numerical model. For this purpose, the deformation charts obtained from the measurements were considered as the main guide. The elastic modulus of the soil was back-calculated using the amount of deformation that occurred during and after the construction of the dam, and also the deformation occurring in one-layer construction of the dam. The mathematical relationship between stress and displacement was established and the values of the elastic modulus were then back-calculated.

This was achieved by calculating the effect of the construction of each layer with specific thickness and by adding the produced stress value of each layer to the layers below. Due to the deformations that occur as a result of the increase in the amount of the stress, the equation of the elasticity modulus (Eq. (1)) could be established.

$$\sigma = E \times \varepsilon \tag{1}$$

In Eq. (1), σ is the stress, E is the modulus of elasticity, and ε is the strain.

Assuming a linear behavior for the materials, elastic modulus E of each layer was calculated with very good accuracy. The value of E was then back-calculated for every layer in the middle section of the dam and eventually, the average value of E was calculated. This value was then compared with the value of the elastic modulus that was considered in the initial design. The ratio of these two values is a very good approximation that can be extended to other parts of the rock-fill materials in the dam. To find the best value for this ratio, the initial moduli of elasticity of the materials were reviewed for every layer and the numerical analyses were repeated. The results were then compared with the results of the measurements.

To calculate the values of the elastic modulus from the results of the measurements a number of points were selected on the magnetic settlement curves and the height and the settlement of these points were recorded. Note that these values resulted from the construction of the upper layers. Having the exact values of the soil unit weight used in the dam (obtained from in-situ tests that were performed during implementation of the dam body) and the thickness of each of the constructed layers, the induced stress values were calculated. Dividing this by the deformations that occurred as a result of the construction of the upper layer, the corrected values of the elastic moduli were obtained. These calculations are shown in Table 3. The average modulus of elasticity was found to be equal to 120 MPa. By dividing this amount to the initial modulus of elasticity, an average rate of 2.5 was achieved as the initial ratio to revise the old modulus of elasticity.

Table 3 Calculation of the revised modulus of elasticity.

Layer thickness (m)	Δy (mm)	$\gamma\ (\frac{kN}{m^3})$	$\Delta\sigma\ (\frac{kN}{m^3})$	E (MPa)
5.5	4	22.6	124.3	170.91
4.0	5	22.6	90.4	72.32
5.0	7	22.6	113.0	80.71
18.0	7	22.6	406.8	1046.05
9.0	12	22.6	203.4	152.55

The numerical model was then calculated to find the vertical displacement using different ratios for the elastic modulus correction. It was found that a ratio of 2.5 resulted in a risky design, as some of the vertical deformations were calculated lower than the values of the measurements. Therefore, a ratio of 1.5 to 2.0 was considered as a more appropriate value for the correction of the elastic modulus. Figure 9 shows the effect of elastic modulus on the deformation.

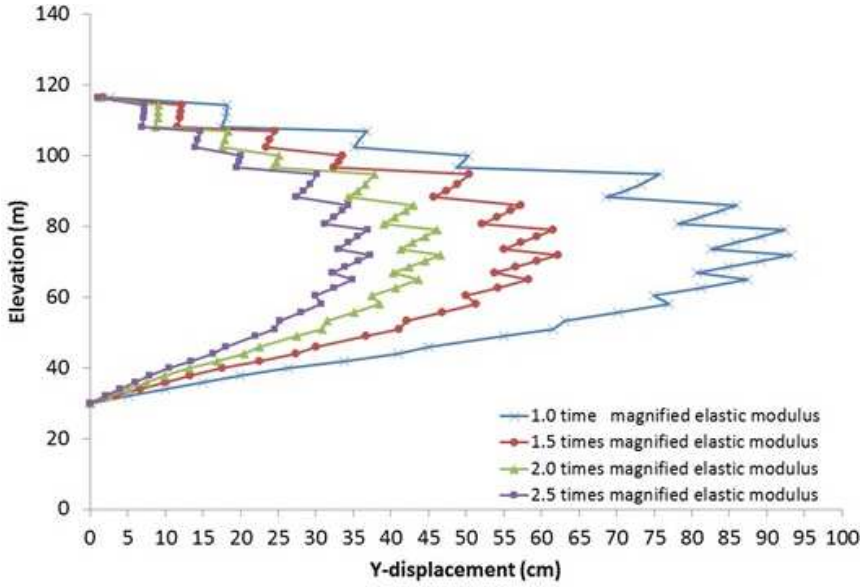

Figure 9 Effect of modulus of elasticity ratio on the vertical deformation on the central line of dam.

Table 4 shows the ratio between the new elasticity modulus and the initial modulus for different materials used in the dam's construction. By performing several analyses and using trial and error, the most appropriate value of the modulus of elasticity was calculated for each layer. These values are presented in Table 5. As can be seen, the initial specifications of the material of the dam body (Zones 3A, 3B and 3C) in the initial analyses (before construction) were considered conservative while the specifications of the layers below the concrete surface (2A and 2B) were selected close to reality.

Figure 10 shows the vertical deformations of the dam's central line after correction of the elastic modulus as an example. As can be seen, the results of the numerical model are consistently close to the displacement recorded by the instrumentation.

Table 4 Ratio of revised elastic modulus to initial modulus.

Material	Initial modulus (MPa)	Modified modulus (MPa)	Ratio
2A	59	55	0.9
2B	45	45	1.0
3A	45	85	1.9
3B	45	85	1.9
3C	30	75	2.5
Alluvial	16	40	2.5
Concrete	5000	5000	1.0

Table 5 Revised specifications of materials.

Zone	Behavior model	E (MPa)	c (kPa)	ϕ°	$\gamma(\frac{kN}{m^3})$	v
2A	E-P*	55	0	42	22.9	0.30
2B	E-P*	45	0	45	22.2	0.30
3A	E-P*	85	0	45	22.2	0.30
3B	E-P*	85	0	45	22.2	0.30
3C	E-P*	75	0	40	21.8	0.30
Alluvial	E-P*	40	0	28	20.9	0.35
Concrete	Elastic	5000	NA	NA	25.0	0.20

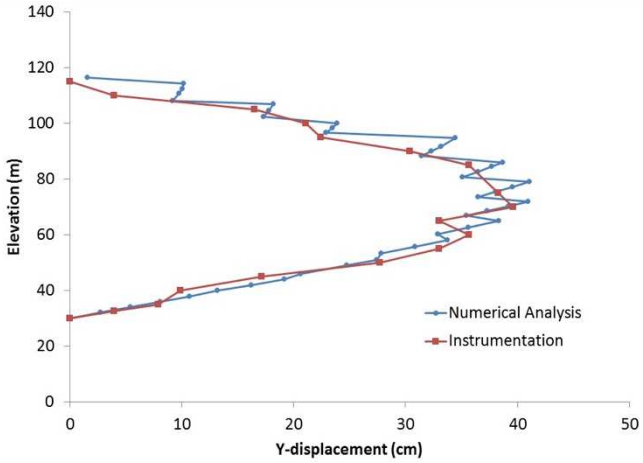

Figure 10 Comparison of vertical deformation of the center line of the dam obtained from numerical modeling (revised material properties) and from measurements.

In addition to the deformations occurring within the dam body due to the weight of the materials, impounding will also cause deformations in the body of the dam, specifically in the sections of the dam that are below the concrete surface. These deformations are perpendicular to the surface and it is important to consider them in the numerical modeling. Since the finite-element software provides the amount of deformation in the nodes in the form of horizontal and vertical deformations, it is necessary to calculate the resultant of these values in the direction perpendicular to the surface. The dam has an upstream slope of 1V:1.6H. Thus, by dividing the values of the calculated horizontal deformation with the sinus of this angle and also dividing the values of the vertical deformation with the cosine of the angle and adding these values together, the deformation perpendicular to the surface was calculated. Figure 11 shows the deformation of the concrete surface as the effect of impounding in the direction

perpendicular to the surface. The results are shown for both the numerical model and the measurement data. It can be seen that the values of deformation for the sections between the heel of the dam and the middle height of the dam are consistently close. However, the results did not change the altitude for the rest of the dam's height. The results of the numerical analysis were compared with some other CFRDs and a trend similar to the results of the numerical model for the deformations was observed. Therefore, the authors believe that the observed inconsistency in Figure 11 is due to errors in reading of the instruments measuring deformation of the concrete surface.

The adaptation percentage of the bottom of the two charts can be calculated as:

$$\text{Adaptation percent} = \left[1 - \frac{21\text{ cm} - 19.5\text{ cm}}{21\text{ cm}}\right] \times 100 = 93$$

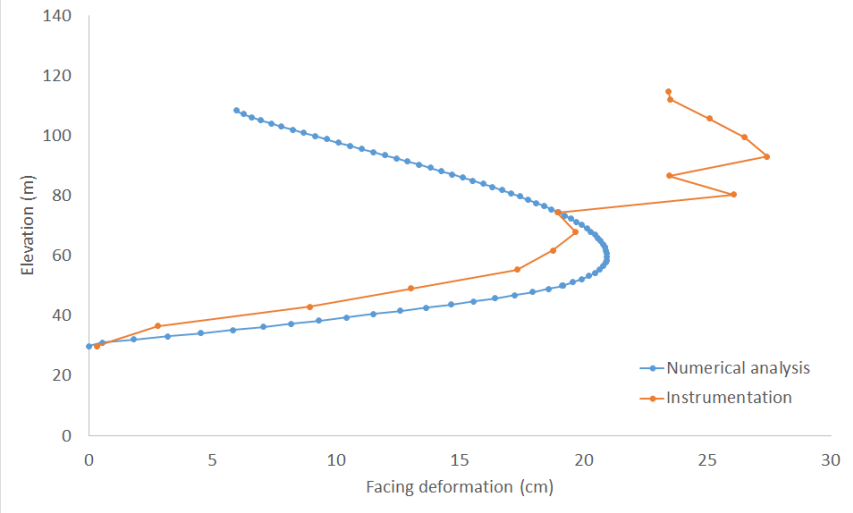

Figure 11 Deformation of the concrete surface of the dam in the direction perpendicular to the surface.

7 Back-Analysis Based on the Elastic Modulus

Applying the final specifications of the materials to the model, analyses were performed for the end of the construction, before and after impounding. Sixteen stages were considered for the construction phase, which means that 16 layers of soil were placed step by step to construct the numerical model. Figure 12 shows the contours of the vertical and horizontal deformations, normal (vertical) stresses, and also the shear stresses within the dam body and after impounding.

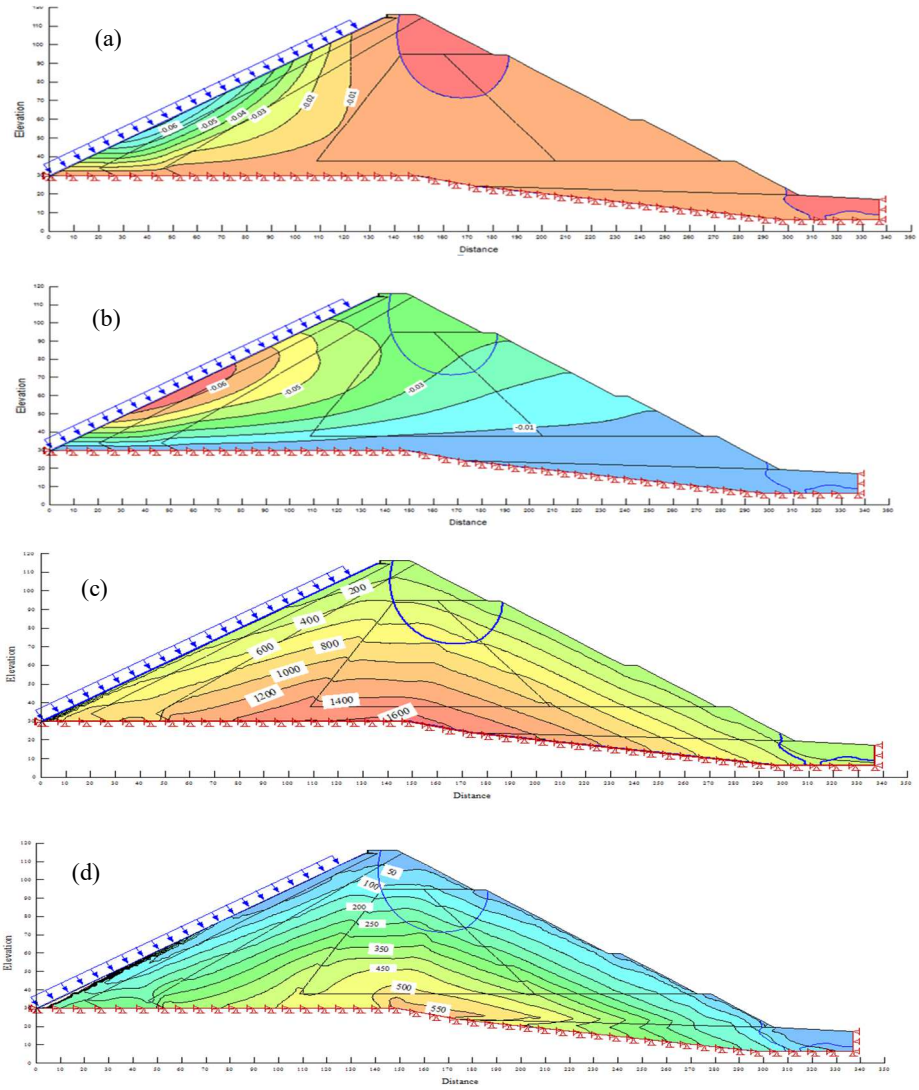

Figure 12 Results of the numerical model with the final revised soil properties: (a) vertical deformations (m), (b) horizontal deformations (m), (c) normal (vertical) stress (kPa), (d) maximum shear stress (kPa).

It can be seen that after impounding, the maximum deformations happen in the parts of the dam that are located directly underneath the concrete surface. In addition, the horizontal deformation will also increase at the upper levels of the dam body. In other words, a large part of the vertical deformations of the main areas of the body will occur due to impounding of the dam rather than due to construction. Also, it can be seen that the effects of impounding on horizontal

deformations are greater than those on vertical deformations. The horizontal displacements would of course decrease the amount of vertical deformation. This can be clearly seen in Figure 12(a) and (b).

It can also be seen in Figure 12(c) and (d) that impounding will increase the normal and maximum shear stresses within the sections of the dam located under the concrete surface. The increase in the values of these stresses is negligible in the middle sections of the dam body. Given that the hydrostatic pressure of water increases linearly with height, the lower level of the surface will have the greatest increase in stress. The results show that the maximum shear stress in the sections underneath the concrete surface will increase from about 100 kPa before impounding to about 1,000 kPa after impounding. The normal stress in the above-mentioned sections will also increase from about 100 kPa before impounding to about 500 kPa after impounding. However, changes in the vertical stress and maximum shear stress in the central areas before and after impounding are smaller than about 50 kPa.

8 Conclusion

Deformation control of a rock-fill body is essential for a high CFRD. The settlement of the Siah-Bisheh CFRD was analyzed based on monitoring records and numerical modeling in this work. A back-analysis method was implemented based on monitored records. The following specific conclusions can be drawn from this study:

1. The differences in the results of the numerical model and the measurements revealed that the initially considered properties of the materials of the primary design were very conservative.
2. Accurately modeling the steps of construction is significantly important and will strongly affect the results of the numerical model. Increasing the number of layers (construction stages) from 5 to 16 in this paper, resulted in varying deformations of up to 30 cm.
3. The results of the back-analysis suggest a considerable change in the value of the elasticity modulus in the middle sections of the dam body. The conversion ratio between the initial elastic modulus and the final elastic modulus of these sections of the dam body was found to be most appropriate at about 2.0. However, the conversion ratio for the materials in the sections under the concrete surface was found to be most appropriate at 1.0.
4. According to the result of back-analysis, for the lower half of the dam height, the deformations of the concrete surface due to the impounding were consistently close to the field measurements.

References

[1] Cook, J.B. & Sherard, J.L., *Concrete Face Rock-Fill Dams-Design*, Construction and Performance, 1st ed., ASCE, pp. 5-7, 1985.

[2] Hunter, G. & Fell, R., *Rock-Fill Modulus and Settlement of Concrete Face Rock-Fill Dams*, J. Geotech. Geoenviron. Eng., **129**(10), pp. 909-917, 2003.

[3] Yang, Z.Y. & Jiang, G.C*., Deformation Control Techniques for 200 M-High Hongjiadu Concrete Face Rock-Fill Dam*, Chin. J. Geotech. Eng., **20**(8), pp. 1241-1247, 2008.

[4] Zhou, W., Chang, X.L., Zhou, C.B. & Liu, X.H., *Creep Analysis of High Concrete-Faced Rock-Fill Dam*, 1st ed., Commun. Numer. Meth. Eng., pp. 1477-1492, 2009.

[5] Szostak, A. & Massiéra, M., *Relation Between Monitoring and Design Aspects of Large Earth Dams*, In: 3rd IAG/12th FIG Symposium, Baden, pp. 22-24, 2006.

[6] Li, J.C., *Gouhou Dam and Analysis for Causes of the Dam Failure*, Chin J. Geotech. Eng., **16**(6), pp. 1-14, 1994.

[7] Cook, J.B., *Process in Rock-fill Dams, The 18th Terzaghi Lecture*, J. Geotech. Eng., ASCE, **110**(10), pp. 1383-1414, 1984.

[8] Li, N.H., *New Concept of Design for High Concrete Face Rock-Fill Dams*, Chin. J. Geotech. Eng., **29**(8), pp. 1143-1150, 2007.

[9] Jing, L., *A Review of Techniques, Advances and Outstanding Issues in Numerical Modelling for Rock Mechanics and Rock Engineering*, Int. J. Rock. Mech. Mining. Sci., **40**(4), pp. 283-353, 2003.

[10] Hua. J.J., Zhou. W., Chang. X.L. & Zhou. C.B., *Study of Scale Effect on Stress-Deformation of Rock-Fill*, Chin. J. Rock. Mech. Eng., **29**(2), pp. 328-335, 2010.

[11] Cetin, H., Laman, M. & Ertunc, A., *Settlement and Slaking Problems in the World's Fourth Largest Rock-Fill Dam*, the Ataturk Dam in Turkey, Eng Geol, **56**(1), pp. 225-242, 2000.

[12] Szostak-Chrzanowski, A., Chrzanowski, A. & Massie, M., *Use of Deformation Monitoring Results in Solving Geomechanical Problems – Case Studies*, Eng. Geol., **79**(1), pp. 3-12, 2005.

[13] Yu, Y.Z., Zhang, B.Y. & Yuan, H.N., *An Intelligent Displacement Back-Analysis Method for Earth-rock-fill Dams*, Comput. Geotech., **34**(1), pp. 423-434, 2007.

[14] Gikas, V. & Sakellariou, M., *Settlement Analysis of the Mornos Earth Dam (Greece): Evidence from Numerical Modeling and Geodetic Monitoring*, Eng. Struct., **30**(1), pp. 3074-3081, 2008.